Proceedings of the Korean Nuclear Society Spring Meeting
Cheju, Korea, May 1996

Dynamic Strain Aging on the Leak-Before-Break Analysis in SA106 Gr.C Piping Steel

Jin-Weon Kim and In-Sup Kim
Korea Advanced Institute of Science and Technology

Abstract

The effect of dynamic strain aging (DSA) on the leak-before-break (LBB) analysis was estimated through the evaluation of leakage-size-crack and flaw stability in SA106 Gr.C piping steel. Also, the results were represented as a form of "LBB allowable load window". In the DSA temperature region, the leakage-size-crack length was smaller than that at other temperatures and it increased with increasing tensile strain rate. In the results of flaw stability analysis, the lowest instability load appeared at the temperature corresponding to minimum J-R curve which was caused by DSA. The instability load near the plant operating temperature depended on the loading rate of J-R data, and decreased with increasing tensile strain rate. These are due to the strain hardening characteristic and strain rate sensitivity of DSA. In the "LBB allowable load window", LBB allowable region was the narrowest at the temperature and loading conditions where DSA occurs.

1. Introduction

The leak-before-break (LBB) concept has been applied to design for high energy piping in nuclear power plant. The stress-strain curve and J-R curve of material are used for LBB analysis, and they have direct influence on the evaluation of LBB conditions [1]. Accordingly, it can be expected that the characteristics of dynamic strain aging (DSA) in material may influence the results of LBB analysis, since the occurrence of DSA depends on temperature and deformation rate and changes mechanical properties.

Although a number of studies on DSA related to LBB were reported [2,3,4], most of them focused on the crack jump at quasi-static loading rate and on the loss of fracture toughness under dynamic loading at the normal plant operating temperature. The effect of DSA on the results of LBB assessment has not been quantitatively estimated. In this study, therefore, the effect of DSA on the LBB analysis was estimated through the evaluations of leakage-size-crack and flaw stability for simple case using material properties obtained from systematic tensile and J-R tests.

2. Material Properties for LBB Analysis

The calculations of leakage-size-crack length and flaw stability in LBB analysis require the stress-strain curve and J-R curve [5]. The tensile and J-R tests were carried out under various temperature and loading conditions to illustrate the characteristics of DSA. In the results, the effect of DSA on the material properties for LBB analysis was clarified. On the basis of this understanding, the sets of material properties to identify the DSA effect were

selected as input data for evaluation. The material used in test was SA106 Gr. C steel which has been used for main steam line piping in nuclear power plant.

In order to use the J-R data to the flaw stability analysis, the J-R curves were fitted to an offset power-law equation as given by [6]

$$J = J_i + C\Delta a^m \tag{1}$$

where J_i is the initiation toughness, C and m are fitting parameters. The fitting parameters obtained from the regression of data points between 0.5 and 2.5 mm in crack extension. The parameters J_i, C, and m are given in Table 1. To obtain the Ramberg-Osgood parameters employed in the calculations of leakage-size-crack and flaw stability, all true stress-strain curves were fitted by using following relation.

$$\frac{\varepsilon}{\varepsilon_o} = \frac{\sigma}{\sigma_o} + \alpha\left(\frac{\sigma}{\sigma_o}\right)^n \tag{2}$$

where σ and ε are true stress and true strain, σ_o is reference stress that is usually equal to σ_{ys}, $\varepsilon_o=\sigma_o/E$, n and α are fitting parameters. The stress-strain data between $1.05\sigma_{ys}$ and 10% strain were selected for fitting [1,7]. The resulting parameters and other tensile properties are given in Table 2.

3. LBB Analysis

The evaluation of leakage-size-crack and flaw stability was performed for simple piping system using material data discussed in the previous section. The piping system was assumed circumferencial through wall cracked pipe with dimension of 670 mm outer diameter and 32 mm thickness. It was operated under 7.3 MPa and 289°C steam, and was subjected to remote axial tension and bending moment as shown in Fig. 1.

The calculation of crack length for given leak rate was performed using PICEP code [8]. All calculations were based on the assumptions of a flaw surface roughness of 0.05 mm and an elliptical circumferential crack which plastic-zone was corrected. For a given load level, the crack length that produces the desired 37.85 *l*/min (10gpm) leak rate was determined.

J/T diagram method was employed for evaluation of flaw stability [1]. The elastic-plastic J-integral estimation formula from EPRI NP-6301-D [9], known as the EPRI/GE estimation method, was used in the J and T calculations. This method superposes solutions corresponding to elastic and fully plastic conditions to obtain the elastic-plastic results for through-wall crack in a pipe. For the case of a through-wall crack in a pipe under remote axial tension and bending moment loading, the following J-integral estimation equation is used for the elastic-plastic solution.

$$\begin{aligned} J &= J_e + J_p \\ &= f_t \cdot \frac{P^2}{4Rt^2E} + f_b \cdot \frac{M^2}{R^3t^2E} + \alpha\sigma_0\varepsilon_0 R(\pi-\theta)\cdot\left(\frac{\theta}{\pi}\right)\cdot h_1 \cdot \left(\frac{P}{P_0}\right)^{n+1} \end{aligned} \tag{3}$$

The individual terms are as described in detail in Reference [9]

4. Results and Discussion

4.1 Effect of DSA on the Leakage-Size-Crack

Fig. 2 shows the dependence of leakage-size-crack length on temperature and strain rate of material properties. The crack length at room temperature (RT) was the largest. The smallest crack length for same load level was observed at 296°C rather than at 400°C. The variation in crack length was not linear with temperature, particularly it was clear at 1.39×10^{-4}/s. The crack length increased with increasing σ_{ys} and n, and with decreasing α. The role of σ_{ys} and n is dominant. Accordingly, the largest value of σ_{ys} and n at RT is a cause of maximum crack length. Although the value of σ_{ys} at 296°C is larger than that at 400°C, the crack length at 296°C is smaller. This is owing to small n at 296°C associated with DSA in tensile properties.

In comparing the leakage-size-crack length with strain rate at each temperature, at 296°C crack length for 6.95×10^{-2}/s was larger than that for 1.39×10^{-4}/s, whereas crack length at 1.39×10^{-4}/s was larger than that at 6.95×10^{-2}/s for other temperatures. The variation in σ_{ys} and α with strain rate at same temperature is small compared with that in parameter n except for data at RT. Therefore, the inverse trend of crack length with strain rate at 296°C relates to the changing of dependence of n on strain rate in the DSA region. Consequently, the strain hardening characteristic of DSA results in a decreased leakage-size-crack length at 296°C, and the negative strain rate dependence in DSA region is a cause of increasing leakage-size-crack length with increasing strain rate.

4.2 Effect of DSA on the Flaw Stability

The effect of loading rate in material properties on the instability load for a given crack length, $2\theta_c/C=0.1$, was represented in Fig. 3 as a function of temperature. It showed that the variation of instability load with temperature was similar to that of J-R curve for each loading rate. The minimum load appeared at a certain range of temperature which depends on loading rate of J-R data. It shows that a decrease in J-R curve caused by DSA alters instability load significantly, although the crack driving force of J-applied decreases due to the enhanced tensile properties and balances out the decrease in J-material [10].

Also, the effect of strain rate of tensile data on the instability load was observed. In the temperature below 200°C, the instability load at 1.39×10^{-4}/s was smaller than that at 6.95×10^{-2}/s. Between 200 and 296°C, however, the trend of variation with strain rate was reversed. According to the results of parametric study, the instability load for a given crack length increased with increasing σ_{ys}, and with decreasing α and n. In the lower temperature region, therefore, an increase in instability load with strain rate is due to high value of σ_{ys}. However, the variation of σ_{ys} with strain rate is negligible between 200 and 296°C, while the value of n increases with increasing strain rate. Accordingly, a decrease in instability load with strain rate is caused by high value of n at high strain rate in this temperature region. The disappearance of strain rate sensitivity of σ_{ys} and positive strain rate sensitivity in n are characteristics of DSA in the tensile properties.

Because of the characteristics of DSA in the material properties, the minimum instability load occurs near the nuclear power plant operating temperature, and the temperature corresponding to minimum load depends on loading rate of J-R data. In addition,

the DSA decreases instability load with increasing strain rate of tensile data in this temperature region.

4.3 LBB Allowable Load Window

Figs. 4 and 5 represent the effects of DSA on the LBB analysis as a form of "LBB allowable load window" [11]. The band between the minimum moment to produce desired leakage rate and the maximum-allowable-moment for a given crack length is LBB acceptable region. In these figures, the safety factor for leakage-size-crack length and applied load was not applied. Fig. 4 shows the LBB allowable region as a function of temperature of material properties at quasi-static loading condition. The LBB allowable region at 250 and 296°C were decreased by about 30% compared with that at RT or 350°C. It reflects that DSA reduces LBB allowable region significantly. Fig. 5 exhibits the LBB allowable region with various combinations of tensile data with J-R data at 296°C, near the plant operating temperature. The variation of LBB allowable region with loading rate of J-R data was considerable, whereas the influence of strain rate in tensile data was negligible. LBB allowable region at loading rate of 4.0mm/min in J-R data was smaller, about 15%, than that of 0.4mm/min for same strain rate. As shown in Fig. 5, LBB allowable region depends on the loading rate of material data at plant operating temperature. However, it is very difficult to know loading rate for practical piping system with certainty. In order to obtain the conservative results in the LBB assessment, the effects of loading rate on the material behavior have to be investigated and then the loading condition corresponding to lower bound material properties should be used for material test.

5. Conclusions

1. The leakage-size-crack length in the dynamic strain aging (DSA) region was smaller than that at other temperatures. Also, DSA increased the crack length with increasing strain rate. These are due to the strain hardening characteristic and negative strain rate sensitivity of DSA in tensile properties.

2. The instability load reduced in the DSA region, and the temperature corresponded to a minimum load depended on loading rate of J-R data. In this region, the instability load decreased with increasing strain rate of tensile properties. This is owing to a decrease in fracture toughness, a disappearance of strain rate sensitivity of σ_{ys}, and an enhancement of strain hardening caused by DSA.

3. Leak-before-break (LBB) allowable region in the range of DSA was decreased by about 30% compared with that in other region of temperatures. Also, it varied with loading rate of material data at plant operating temperature.

References

[1] NUREG-1061, Vol.3, October 1984.
[2] B. Mukherjee, Nucl. Eng. & Des. 111, 1989, p63.
[3] C. W. Marschall, M. P. Landow and G. M. Wilkowski, NUREG/CR-6098, October 1993.

[4] C. W. Marschall, R. Mohan, P. Krishnaswamy and G. M. Wilkowski, NUREG/CR-6226 October 1994.
[5] B. F. Beaudoin, D. F. Quinones and T. C. Hardin, J. Pres. Ves. & Piping 43, 1990, p67.
[6] G.M. Wilkowski, G. Karmer, P.Vieth, R. Francini, and P. Scott, *PVP-Vol.280*, ASME 1994, p221.
[7] M. L. Vanderglas, Int. J. Pres. Ves. & Piping 43, 1990, p241.
[8] D.M. Norris and V. Chexal, *PICEP, EPRI NP-3596-SR*, Dec. 1987.
[9] A. Zahoor, *EPRI NP-6301-D*, Vol.1, June, 1989.
[10] O. E. Lepik, B. Mukherjee, Int. J. Pres. Ves. & Piping 43, 1990, p285.
[11] A.D. Nana and K.K.Yoon, *PVP-Vol.287/MD-Vol.47*, ASME, 1994, p35.

Table 1 Parameters of J-R curves obtained from power-law fitting(Δa = 0.5~2.5 mm).

Loading Rate	Temp. (°C)	J_i (kJ/m^2)	C	m
0.4 mm/min	RT	153.44	464.7	0.7899
	150	115.23	425.0	0.7626
	200	97.95	415.5	0.6841
	250	102.53	363.4	0.6403
	296	131.68	377.9	0.6910
	350	148.60	517.1	0.8302
4.0 mm/min	RT	175.74	483.2	0.7604
	150	146.42	484.4	0.6957
	200	118.85	438.1	0.7420
	250	108.96	393.3	0.6479
	296	109.55	352.5	0.6125
	350	210.28	352.5	0.6889

Table 2 Tensile properties employed in the evaluations of the leakage-size-crack and flaw stability analysis.

Srain Rate	Temp.(°C)	σ_{ys}(MPa)	σ_{uts}(MPa)	α	n
1.39×10^{-4}/s	RT	331	540	5.8903	4.1685
	150	272	504	5.2406	3.8648
	200	255	536	4.6039	3.5341
	250	253	555	3.9109	3.5012
	296	242	562	3.8894	3.3738
	350	235	521	3.4455	3.5533
	400	226	438	2.6259	4.4629
6.95×10^{-2}/s	RT	362	575	6.7979	3.8817
	150	323	503	6.1191	4.3611
	200	294	482	5.9687	4.1888
	250	265	478	5.4656	3.8577
	296	245	499	4.0332	3.7095
	350	234	511	3.3037	3.6336
	400	233	501	3.1845	3.7230

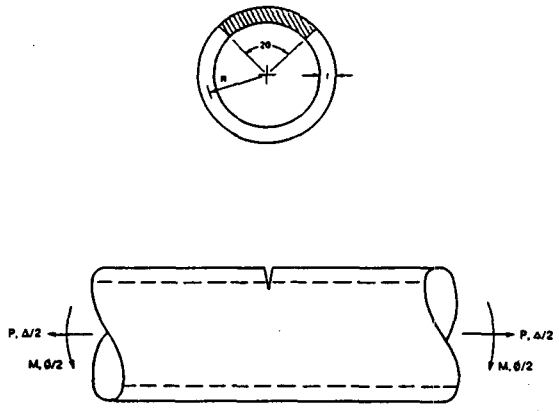

Fig. 1 Circumferential throughwall-cracked in a pipe and applied loads.

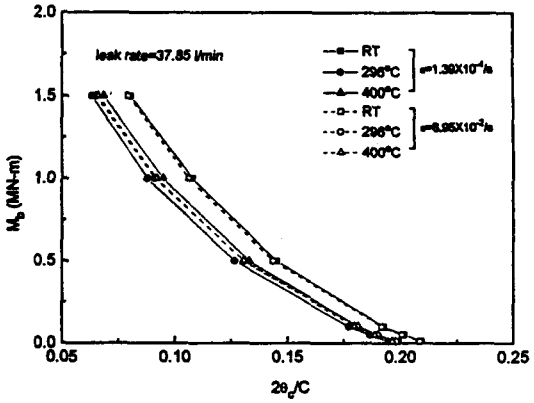

Fig.2 Minimum bending moment versus leakage-size-crack length calculated by PICEP code.

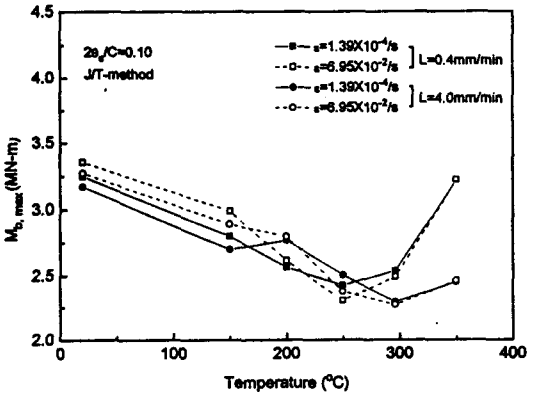

Fig. 3 Effect of temperature and loading rate of material data on the instability load for $2\theta_c/C$=0.1.

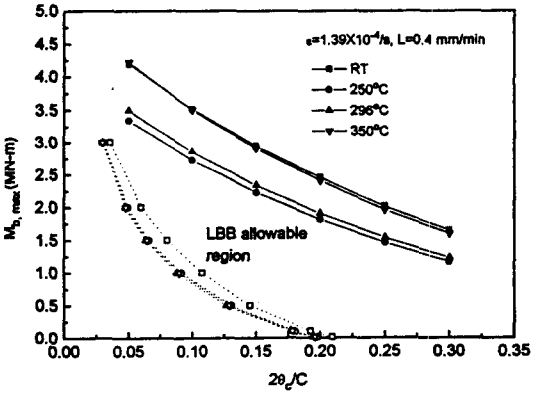

Fig. 4 Variation in LBB allowable region with temperature of tensile and J-R data at quasi -static loading rate.

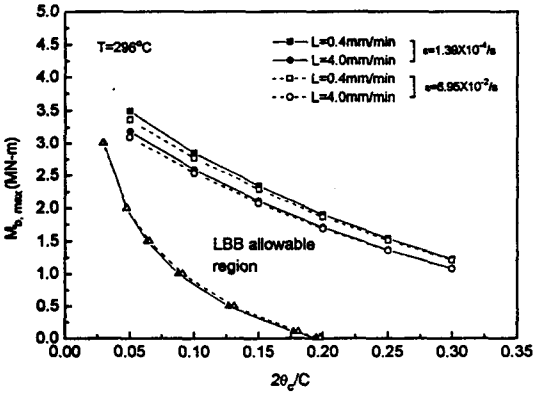

Fig. 5 Variation in LBB allowable region with loading rate of tensile and J-R data at 296°C.